Comparative Biochemistry and Physiology, Part A 308 (2025) 111904

Contents lists available at ScienceDirect

Comparative Biochemistry and Physiology, Part A

journal homepage: www.elsevier.com/locate/cbpa

Research Article

Hypoxia impairs survival and alters immune and iron metabolism gene expression during shark early ontogeny

Sandra Martins [a,b,*], Jaquelino Varela [a,c], Rute Felix [b,1], Catarina Pereira Santos [a,c], José Ricardo Paula [a,d], Deborah M. Power [b], Rui Rosa [a,c,d,*]

[a] MARE – Marine and Environmental Sciences Centre / ARNET – Aquatic Research Network, Laboratório Marítimo da Guia, Faculdade de Ciências, Universidade de Lisboa, Cascais, Portugal
[b] Comparative Molecular and Integrative Biology, Centro de Ciências do Mar, Universidade do Algarve, Faro, Portugal
[c] Sphyrna Association, Boa Vista Island, Sal Rei, Cape Verde
[d] Departamento de Biologia Animal, Faculdade de Ciências, Universidade de Lisboa, Cascais, Portugal

ARTICLE INFO

Editor: Michael Hedrick

Dataset link: Gene expression of immune and neuroendocrine-related genes and biometric data of small-spotted catshark embryos (Scyliorhinus canicula) after six days of exposure to deoxygenation and hypoxia (Original data)

Keywords:
Deoxygenation
Embryos
Endocrinology
Hypoxia
Immunology
Scyliorhinus canicula
Sharks

ABSTRACT

The global oxygen inventory has been declining worldwide, primarily due to climate change. The importance of oxygen for aerobic respiration and its homeostasis makes declining oxygen levels a concern, particularly during energy demanding lifecycle stages. The effects of low oxygen levels on neuroendocrine responses and immune competence of developing sharks were studied in the head and trunk tissues of early (EE; before pre-hatching) and late embryos (LE) of small-spotted catshark (*Scyliorhinus canicula*) under six days of deoxygenation (93 % O_2 of air saturation) and hypoxic conditions (26 % O_2). Catshark embryos were resilient to deoxygenation, with only a 10 % decline in survival compared to the control, and only the gene expression of melanotransferrin changed. Under hypoxia, growth was unaffected, but survival decreased by 31 % compared to the control in LE, highlighting an inadequate physiological response. Developmental stage affected the expression of hypoxia-inducible factor 1 alpha (*hif1a*), iron metabolism and immune-related genes, pointing to critical response mechanisms. The EE stage had an optimised stress response under hypoxia compared to LE, with the upregulation of the *hif1a* gene. The lack of a protective response and compromised immune-related functions under hypoxia in LE raise concerns about species survival under climate change. These findings highlight the need for further research on the likely resilience of sharks to environmental challenges.

1. Introduction

There is a growing consensus that between 1970 and 2010, the open ocean lost 0.5–3.3 % of its oxygen, and it is projected to decline by up to 3.7 % more by the end of the century (IPCC, 2023; Laffoley and Baxter, 2019). Global warming is considered the primary cause of deoxygenation due to its effects on the physical properties of water and the respiration rates of marine microbes and animals (Breitburg et al., 2018; Limburg et al., 2020). Furthermore, warming enhances water stratification, which reduces the mixing of water layers and prevents sufficient reaeration of the bottom waters (Breitburg et al., 2018; Laffoley and Baxter, 2019; Limburg et al., 2020). A reduction by up to 98 % of deep ocean circulation will affect the supply of nutrients, the production of organic matter, and its subsequent sinking from the surface ocean (Breitburg et al., 2018; IPCC, 2023; Laffoley and Baxter, 2019). Lastly, eutrophication, caused by nutrient discharge into coastal waters, consumes oxygen and induces hypoxia when oxygen consumption by phytoplankton exceeds its replacement (Breitburg et al., 2018; Limburg et al., 2020).

Ocean model simulations project a decline in the *oxygen content of global oceanic and coastal waters* (deoxygenation) by *up to* 7 % by the end of the century (*IPCC*, 2019; Laffoley and Baxter, 2019). However, hypoxia occurs when oxygen concentrations fall below the critical levels necessary to sustain marine life, dramatically impacting ecosystems and the biodiversity within them (Breitburg et al., 2018; Laffoley and Baxter, 2019; Limburg et al., 2020). The oxygen level associated with fisheries collapse is referred to as hypoxia and has a proposed threshold of 2 mg O_2 L^{-1} (Vaquer-Sunyer and Duarte, 2008), equivalent to 26 % of air

* Corresponding authors.
E-mail addresses: srmelovm@gmail.com (S. Martins), rarosa@ciencias.ulisboa.pt (R. Rosa).
[1] Present affiliation: GreenCoLab – Associação Oceano Verde and Centro de Ciências do Mar, Universidade do Algarve, Faro, Portugal

https://doi.org/10.1016/j.cbpa.2025.111904
Received 26 May 2025; Received in revised form 9 July 2025; Accepted 9 July 2025
Available online 10 July 2025

saturation.

Fish inhabiting coastal ecosystems do not appear to have developed specific physiological adaptations to hypoxia, contrary to species that inhabit environments where hypoxia occurs frequently (Childress and Seibel, 1998; Dam, 2013; McBryan et al., 2013). Thus, continued ocean warming accompanied by deoxygenation will result in habitat contraction and fragmentation due to diminishing oxygen levels that will not meet the metabolic requirements of animals (Breitburg et al., 2018; Laffoley and Baxter, 2019; Limburg et al., 2020; Rosa et al., 2016). Changes in the environment caused by hypoxia include alterations in the distribution of aquatic animals and may increase their susceptibility to disease and predation by hypoxia-tolerant species (Breitburg et al., 2018; Laffoley and Baxter, 2019). Moreover, pathogen transmission and severity can be enhanced in low-oxygen environments (Limburg et al., 2020). Several studies have reported that insufficient oxygen has consequences for growth, reproduction, survival, feeding, recruitment, abundance, development, metabolism, and susceptibility to other stressors (Aku and Tonn, 1997; Brandt et al., 2011; Breitburg et al., 2018, 1999; Craig and Crowder, 2005; Eby et al., 2005; Roman et al., 2019; Sampaio et al., 2021; Shang and Wu, 2004; Taylor and Miller, 2001; Thomas and Rahman, 2012; Zhang et al., 2014).

Early life stages constitute a vulnerable period of an organism's life cycle since they are less tolerant to stressful environmental conditions (Rosa et al., 2014; Sampaio et al., 2021; Santos et al., 2021). In sharks, a critical stage in embryological development happens when the egg case jelly degrades and is replaced by seawater when the four seawater slits open (Musa et al., 2018). At this pre-hatching stage, the microhabitat of the egg case drastically changes (Musa et al., 2020, 2018), exposing the embryo to the surrounding freely circulating seawater and, therefore, to different conditions and new physiological challenges. Spawning of small-spotted catshark (*Scyliorhinus canicula*) typically occurs in shallow waters, usually in sandy areas where the eggs are laid (Compagno, 1984). These eggs are deposited subtidally or in the lower intertidal zone, attached to substrates such as macroalgae, and this means hatchlings and young sharks typically develop in shallow waters (Compagno, 1984; Ellis and Shackley, 1997). In these coastal systems, developing embryos and larvae will be vulnerable to the more frequent fluctuations in temperature and oxygen content that have been projected (*IPCC*, 2019; Wheeler et al., 2020). Additionally, unlike mobile life stages, oviparous embryos cannot move away from hostile environments (Limburg et al., 2020), making them even more vulnerable to environmental stressors. Since declining oxygen levels disrupt the survival rates, growth patterns, and developmental processes of small-spotted catshark embryos (Diez and Davenport, 1990; Musa et al., 2020; Varela et al., 2023), this may negatively impact the survival and health of this oviparous shark species.

Hypoxia induces stress, which can either enhance or suppress immune competence (Colgan et al., 2020; Greijer et al., 2005; Yada and Tort, 2016). The nervous, endocrine, and immune systems regulate these differing physiological responses through integrated circuits (Yada and Tort, 2016). The immune response to stressors is mediated by both the central and peripheral endocrine system and triggers a feedback response that modulates neuroendocrine signalling (Balasch and Tort, 2019; Barton, 2002; Makrinos and Bowden, 2016; Wendelaar Bonga, 1997; Yada and Tort, 2016). During the activation of the immune system or after infection, energy requirements are increased, and glucocorticoids can modulate energy requirements by modifying the inflammatory response (Khansari et al., 2017; Sapolsky et al., 2000). As a result, immune activity decreases, and immune cells may be catabolised to generate protein and glucose (Khansari et al., 2017; Sapolsky et al., 2000). An integrated response by the neuroendocrine and immune systems is indispensable and crucial for animal integrity, allowing them to modulate their physiological response to pathogens (Khansari et al., 2017; Sapolsky et al., 2000). For this reason, abiotic parameters that interfere with the immune and neuroendocrine systems can modify disease resistance and wound healing, which ultimately impairs survival (Limburg et al., 2020; Virtanen et al., 2023).

Research on the impacts of oxygen deprivation on shark immunology and neuroendocrinology is scarce. In fact, studies of the immune response to hypoxia have mainly focused on adult teleost fishes and involve evaluation of the expression of genes such as interferon Mx, TNFR-α, hsp70, interleukins IL-1β and IL-10, and the cyclooxygenase-2 (cox2) gene (Kvamme et al., 2013; Machado et al., 2018; Methling et al., 2010; Niklasson et al., 2011). Additionally, Wu et al. and Thomas et al. (Thomas et al., 2007; Wu et al., 2003) investigated the potential endocrine-disrupting effect of hypoxia on reproductive hormones. To address the critical knowledge gap regarding the influence of oxygen deprivation on vulnerable developmental stages, this study investigated how deoxygenation and hypoxia may impact the embryonic development of *S. canicula*. The significance of this research lies in its potential to uncover widespread physiological changes triggered by these stressors, particularly through the activation of distress-induced genes and alterations within the immune-neuroendocrine axis (Balasch and Tort, 2019; Gorissen and Flik, 2016). In this context, we selected a panel of genes to provide an integrative view of the molecular adjustments occurring during critical developmental windows. These genes encompass those associated with innate immunity, neuroendocrine activation (such as precursors of stress-related hormones), and growth and metabolic regulation (growth pathway and thyroid axis); genes related to energy homeostasis to explore potential shifts in metabolic trade-offs, as well as those involved in the adaptive response to hypoxia. The selected target genes and biometric data were analysed in the head and trunk samples of early (EE) and late (LE) small-spotted catshark embryos exposed to short-term (six days) deoxygenation (D; 93 % of air saturation) and hypoxic (26 % of air saturation) conditions. The study provides important insights into understanding how key marine species, that preserve the intricate balance within marine ecosystems, respond to modified oxygen availability and provides the basis for future conservation strategies in a rapidly changing ocean environment.

2. Material and methods

2.1. Ethics statement

All procedures were reviewed and approved by the Ethics Committee of the Faculty of Sciences of Lisbon University (ORBEA, Statement 2/2021) and conducted in accordance with the requirements of the European Parliament's legal regulations (EU Directive 2010/63).

2.2. Animal collection and acclimation

From November 2021 until January 2022, small-spotted catshark (*Scyliorhinus canicula*) embryos were obtained from two sources and maintained in Laboratório Marítimo da Guia (LMG - Cascais, Portugal). Eight eggs were from a public aquarium, Aquário Vasco da Gama (AVG, Algés, Portugal), where captive *S. canicula* females laid them. The remaining 26 eggs were the descendants of four female and two male catsharks caught by fishermen using traps at Figueira da Foz (Portugal) in February of 2021, maintained in LMG and allowed to breed. Egg deposition was checked daily in LMG and AVG, and when females laid a pair of eggs (one from each oviduct), they were collected, identified with the deposition date, and transferred to an acclimation tank in LMG. The 34 eggs were acclimated for at least 30 days in a 600 L tank in a semi-closed life support system (1080 L total seawater volume). The semi-closed life support system was fed by 0.35 μm filtered (Harmsco, USA) and UV-irradiated natural seawater (Vecton 300, TMC Iberia, Portugal). Water quality was maintained using biological filtration [i.e., Ouriço® bio balls (Fernando Ribeiro, Portugal), fluidised sand bed filters (FSBF 1500, TMC Iberia, Portugal)] and protein skimmers (Schuran, Germany). The seawater temperature was regulated automatically with temperature controllers (T controller twin, Aquamedic, Germany) connected to chillers (Hailea, China) and thermostats (V^2 Therm 100, TMC

Iberia, Portugal).

Physicochemical water conditions were set to 16 °C, 8.0 pH units, 33 g L^{-1} of salinity, and 100 % oxygen with CO_2-filtered air (using soda lime, Sigma-Aldrich, Germany). A photoperiod with a cycle of 12 h light/12 h dark was provided by artificial illumination. The intensity of illumination was consistent across treatments throughout the experiment. Each group of progenitors (two females and one male) was maintained in a 600 L tank belonging to a 1080 L semi-closed system with the same water quality conditions as the embryo's acclimation tank. Temperature, pH, and dissolved oxygen were manually monitored daily using a WTW Multi 3510 IDS SET 4 with a pH-electrode SenTix® 940 (WTW, Germany) and a dissolved oxygen sensor FDO® 925 (WTW, Germany), and salinity was verified using a water salinity tester Hanna HI98319 (Hanna Instruments Portugal, Lda). Ammonia (NH_3/NH_4^+) and nitrite (NO_2^-) were monitored in the circuit water using colorimetric test kits (Tropic Marin, Switzerland) every week and kept below detectable levels. One week before the beginning of the experiment, the eggs were randomly assigned to a treatment.

2.3. Experimental conditions

To assess the effect of oxygen loss (Laffoley and Baxter, 2019), experiments took into account (*IPCC*, 2019) projections and the definition of hypoxia (oxygen levels below 2 mg L^{-1}) (Vaquer-Sunyer and Duarte, 2008). Three experimental treatments were established: *i*) control (100 % air saturation), *ii*) deoxygenation (D; 93 % of air saturation), and *iii*) hypoxia (26 % of air saturation). A Loligo ® Online Oxygen Converter was used to convert the percentage of air saturation into oxygen content.

A sample size calculation for this study with a set statistical power was not possible due to the absence of effect size data from previous studies, and the lack of realistic estimates of the expected effect size and variability of *S. canicula* embryos' responses. For this reason, the 3R framework was followed, prioritizing the humane use of the animals. The authors have extensive experience in maintaining this species under laboratory conditions (Martins et al., 2024; Pegado et al., 2020a, 2020b; Varela et al., 2023), and the experimental protocols were previously refined.

34 embryos of between 42- (early embryos; EE) and 111-days (late embryos; LE) post-laying (dpl) were randomly allocated to each treatment, and three replicate tanks per treatment were established (Table S2). Each treatment had three semi-closed recirculating systems with a drip system equipped with protein skimmers (Reef Skim Pro 400, TMC-Iberia, Portugal), biological filtration (Ouriço® bio balls, Fernando Ribeiro, Portugal), and automatic temperature control (XH-W3002 controller, hysteresis 0.3 °C) connected to water heaters (Eheim thermocontrol 150, Eheim GmbH & Co KG, Germany) and a water chiller (Hailea HC-150 A). Deoxygenation and hypoxia treatments had an individual cylindrical column where certified nitrogen gas (Air Liquide, Portugal) was injected into seawater via a solenoid valve. Each replicate tank was continuously fed with oxygen-limited seawater with a pump (35 W; TMC, V2 Power Pump, 2150 L h^{-1}). Each treatment tank had independent optometers (PyroScience FireStingO2, accuracy ±0.1 mg O_2 L^{-1}), and oxygen levels were monitored and corrected every two seconds. Oxygen saturation levels were controlled using an Arduino Mega controller (Mucha, 2023) with hysteresis set at 0.2 mg O_2 L^{-1}, downregulated by injection of nitrogen gas or upregulated by aeration with CO_2-filtered air (using soda lime, Sigma-Aldrich, Germany) connected to an air compressor (Medo Blower LA-120 A, Nitto Kohki, Japan).

Each replicate was composed of a 45 L tank (56 × 39 × 28 cm), under a photoperiod of 12 h/12 h L:D (light: dark cycle), where egg cases were hung vertically by their tendrils with the arched end facing upwards. Each replicate had an independent supply of filtered (0.35 μm, Harmsco, USA) and UV-irradiated (Vecton 300, TMC Iberia, Portugal) seawater. The seawater flow was adjusted manually each day through an acrylic flow meter (1–10 L min^{-1} range). Salinity, oxygen levels, temperature, pH, NH_3, NH_4^+, and NO_2^- levels were monitored as outlined above.

Experimental exposure of embryos was performed after oviposition continuously for six days. Experimental treatments were as follows: *i)* control with the following seawater conditions, $T = 16.3 \pm 0.2$ °C, pH = 8.07 ± 0.02 pH units, salinity = 33.0 ± 0.2 g L^{-1}, and oxygen saturation = 99.56 ± 0.69 % (n = 11; 3–4 embryos/replicate); *ii)* Deoxygenation (D), $T = 16.1 \pm 0.2$ °C, pH = 8.07 ± 0.02 pH units, salinity = 33.0 ± 0.2 g L^{-1}, and oxygen saturation = 92.83 ± 0.93 % (n = 10; 3–4 embryos/replicate), and *iii)* hypoxia (H), T = 16.3 ± 0.1 °C, pH = 8.16 ± 0.02 pH units, salinity = 33.0 ± 0.2 g L^{-1}, and oxygen saturation = 28.26 ± 3.25 % (n = 13; 4–5 embryos/replicate).

2.4. Biometry and sample collection

An elasmobranch egg case consists of the collagenous egg case membrane, jelly, egg yolk, and the developing embryo (Musa et al., 2018). A total of 34 small-spotted catshark egg cases [$n_{control}$ = 11 (3 EE + 8 LE); n_D = 10 (4 EE + 6 LE); n_H = 13 (4 EE + 9 LE)] were removed from the experimental tanks after six days of exposure. The egg cases were transferred to 90 mm Corning™ Petri dishes (Fisher Scientific, Portugal) filled with seawater from the respective treatment tank, and, under candling, the developmental stage of each embryo was assessed according to the scale of Musa et al. (2018). The egg case was cut at one edge, and the embryo was euthanised by immersion in a solution containing 1 g L^{-1} ethyl 3-aminobenzoate methanesulfonate (Tricaine MS-222; E10521, Sigma-Aldrich) buffered with 1 g L^{-1} sodium bicarbonate (S5761, Sigma-Aldrich). Next, the yolk stalk was cut as near as possible to the embryo's belly with dissecting scissors, detaching the embryo from the egg yolk. The embryo wet mass was recorded using a Sartorius balance (CPA225D, Germany). The total length was measured (from the tip of the snout to the tip of the tail) to calculate Fulton's condition factor (K), which was determined using the total mass (g) divided by the total length (cm) cubed × 100 (Ricker, 1975). The embryo was dissected into two parts: head from the tip of the head to the end of the gills (H), and trunk region (T) from the pectoral to the anal fin (excluding gills), which were then immediately placed in dry ice and stored at −80 °C until RNA extraction.

2.5. Developmental stage characterisation

The developmental status of each embryo in the different treatment regimens was assessed using the scale developed by Musa et al. (2018) under candling and was confirmed visually after euthanasia. EE and LE were selected, and stage four was used as the cut-off (pre-hatching) (Fig. 1, Table S2).

Stage four is a critical point in embryonic development as it marks the moment when embryos are in transition to acquire a state that allows them to cope with exposure to the physicochemical conditions of their habitat. The egg case is inherently porous and has an intricately ordered structure that acts as a selective filtration membrane, enabling respiratory and metabolic exchange (Goh et al., 2021), and the egg case jelly protects embryos from elements in their habitat that cause dehydration (Musa et al., 2018). After stage four, the jelly degrades and is replaced by seawater, and all four seawater slits are fully opened (Musa et al., 2018). This process is termed pre-hatching, exposing the embryo to the surrounding seawater and, therefore, to different conditions and new physiological challenges.

2.6. Analysis of gene expression by quantitative real-time PCR (qPCR)

Total RNA was extracted from shark EE and LE using an E.Z.N.A. ® Total RNA Kit I Protocol (SKU: R6834–02, Omega Bio-tek, Inc.) with 2-mercaptoethanol (A1108,0100, PanReac), following the optimised manufacturer's protocol. In brief, dissected embryos (approximately 150 mg of the head and 100 mg of the trunk) were placed in lysis buffer with two metal beads and disrupted in a Retsch MM400 (Scansci) using

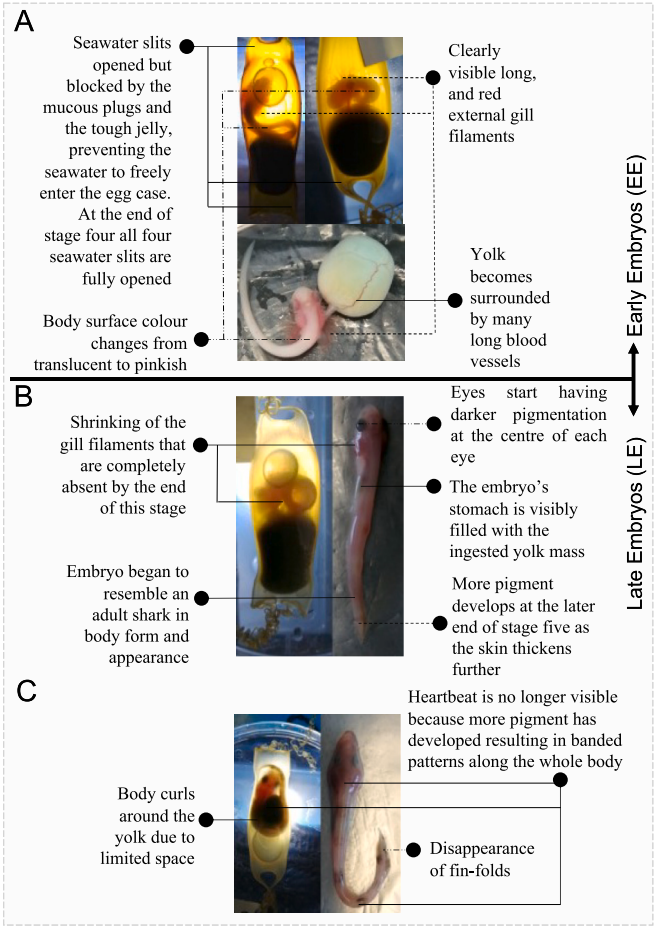

Fig. 1. Characterisation of developmental stages of small-spotted catshark *Scyliorhinus canicula* embryos used in the experiment, according to Musa et al. (2018) (pictures acquired by the authors). Early embryos (EE): A – Stage four (before pre-hatching); Late embryos (LE): B – Stage five, and C – Stage six.

four cycles of 30 s. Total RNA was eluted from the purification columns of the Total RNA kit (E.Z.N.A.) using 30 μL of nuclease-free water, and then any genomic DNA contamination was removed with a Precision™ DNase kit (Primerdesign), following the manufacturer's protocol. The concentration and purity of the extracted RNA were assessed using a NanoDrop ONE © (Thermo Scientific). In head samples, the mean ratios of A260/280 and A260/230 were 1.757 and 1.009, respectively. In trunk samples, the mean for A260/280 and A260/230 ratios was 1.891 and 0.939, respectively. Some samples had low ratios; however, these values were not consistent with both ratios. The high urea contents of marine elasmobranchs (Hazon et al., 2003) (Wood and Giacomin, 2016), the presence of salt from the marine environment and/or proteins (e.g. (Tavares et al., 2011)), and the RNA composition (nucleobase ratios) may have affected the RNA ratios assessed by the NanoDrop. RNA integrity was checked by agarose gel electrophoresis on 0.8 % Seakem® LE Agarose (50,004, Lonza) and run in a PowerPac Basic tray (BioRad). Samples that passed the integrity control were used for gene expression quantification.

Synthesis of cDNA from the extracted total RNA was carried out in a 20 μL reaction volume with 500 ng of total RNA. The reaction conditions were as follows, a preliminary denaturing step at 65 °C for 5 min, followed by the addition of the reagents dNTPs 10 mM, random hexamers 100 μM/200 ng (Jena Biosciences), Ribolock™ RNase inhibitor 40 U/μL (ThermoFisher), and RevertAid™ reverse transcriptase 200 U/ μL (ThermoFisher) and incubation at 20 °C for 10 min, then 42 °C for 50 min, before enzyme heat inactivation at 72 °C for 5 min. The absence of genomic contamination was monitored by PCR amplification of the ribosomal RNA 18S, in extracted RNA. The 18S rRNA PCR was carried out in a 25 μL reaction volume containing 2 μL of total RNA (1:10), dNTPs 10 mM, DreamTaq (VWR), RT4 primers 10 mM (Table S1), and 10 x reaction buffer. The thermocycle was as follows: 95 °C for 5 min, followed by 27 cycles of 95 °C for 20 s, 60 °C for 20 s, 72 °C for 20 s, and a final elongation step at 72 °C for 5 min.

For PCR amplification of the candidate genes cDNA (2 μL of 1:10 dilution) was used. Primers for the candidate genes and reference genes were designed using Primer3, and sequences were retrieved using BLAST against the nucleotide database (NCBI), where the genome of *Scyliorhinus canicula* is available (Table S1). The PCR to detect genomic contamination or the target amplicons was carried out using a T100™ thermal cycler (Biorad). The presence of genomic contamination or candidate gene amplification was checked by agarose gel electrophoresis [(2 % Seakem® LE Agarose (50,004, Lonza)]. In the case of candidate genes, the PCR product was sequenced to confirm primer specificity. The efficiency of each primer was calculated from a standard curve prepared from the isolated and quantified PCR product using five concentrations of a 1:10 dilution series, starting from an initial 1:50 dilution. The standard curves were performed on the same day as the qPCRs.

qPCR was used to quantify the mRNA expression of genes of the neuroendocrine-immune response in control samples and samples from the deoxygenation and hypoxia challenges. To monitor how the loss of oxygen modulated the activity of the neuroendocrine and immune response, the genes ferritin heavy chain (*fer*), melanotransferrin (*meltf*), ferrochelatase (*fch*), lysozyme G-like (*lys*), tumor necrosis factor receptor SF1A associated via death domain (*tnfr*), perforin 1 (*perf1*), interferon regulatory factor 2 (*irf2*), growth hormone receptor (*ghr*), melanin-concentrating hormone receptors 1 and 2 (*mchr1* and *mchr2*), thyroid hormone receptor beta (*thrb*), interferon gamma-like (*ifn*), and nuclear factor kappa B (NFKB) repressing factor (*nfkrf*) were quantified in the shark embryo head and trunk. Growth hormone (*gh*), TSH receptor (*tshr*), proopiomelanocortin a (*pomc*), and thyroid peroxidase *(tpo)* were quantified in the shark embryo head. Because these genes are expressed in the thyroid and pituitary glands (Power et al., 2001), it is irrelevant to quantify them in the trunk. Hypoxia-inducible factor 1 alpha (*hif1a*) was also quantified in both tissues to assess if the embryos had the capacity to recruit hypoxia-protective responses. qPCR reactions were performed in 6 μL reactions containing 1 μL of cDNA (diluted 1:5), 10 μM of each primer, except for the *ifn* primer pair for which a concentration of 5 μM was used, and SsoFast EvaGreen supermix (3 μL, Bio-Rad Laboratories). qPCR was carried out in duplicate reactions in 384 plates prepared using a CyBio® FeliX CHOICE™ robot (AnalytikJena, Germany).

qPCR reactions were carried out in a StepOnePlus qPCR thermocycler, and data were analysed with Bio-Rad CFX Maestro 1.0 software (Bio-Rad Laboratories, USA). Thermocycling conditions were 95 °C for 1 min, 39 cycles of 95 °C for 5 s, and 60 °C for 10 s, followed by a final melt curve between 60 and 95 °C, which gave single product/dissociation curves in all reactions. Two reference genes, ribosomal protein L13 (RPL13) and ribosomal protein S29 (RPS29), which did not vary significantly between treatments and tissues, were used as reference genes. Results were normalised with the geometric mean of these two reference genes. Quantitative gene expression was established using relative quantification, and the results are reported as $2^{-\Delta\Delta CT}$, the fold change in gene expression relative to the control (Livak and Schmittgen, 2001).

2.7. Statistical analysis

All statistical analyses were performed using R Studio software (version 2024.09.0 + 375) on ΔΔCT values. Generalised Linear Mixed Models using Template Model Builder ("glmmTMB" function) were fitted to biometry, survival, and gene expression, with treatment, developmental stage, and tissue as predictor variables. The model residuals were plotted ("check_model" function) to check assumptions of

normality, homoscedasticity, and independence among residuals.

The AIC (Akaike Information Criterion) function was used to determine whether the replicate, treatment, developmental stage, or tissue influenced each response variable, considering the interaction between the variables, and to determine which model was the best fit for the data. Then, type II Wald chi-squared tests (function "Anova") were performed on the models to evaluate the effect of the predictor variables and replicates on each response variable. No significant differences were detected between replicates in any response variable. Post-hoc comparisons between treatments were performed (function "emmeans", package "emmeans") with treatment set as a three-level factor (control, deoxygenation, and hypoxia), developmental stage set as a two-level factor (early and late embryos), and tissue as a two-level factor (head and trunk). The confidence level was set at 0.95, and *p*-values were adjusted through Tukey corrections (Tables S3–4). Variables were plotted using the "ggplot" package on $2^{-\Delta\Delta CT}$ values (the fold change relative to the Control). Principal component analysis (PCA) was performed using the "prcomp" function. Eigenvalues were displayed in a scree plot ("fviz_eig" function), the cumulative variance percentage was confirmed through the "summary" function, and the "fviz_pca" function allowed the visualization of the PCA. The effect size was determined using the package "effsize", function "cohen.d", and the statistical power through function "pwr.anova.test" (Table S5).

3. Results

3.1. Shark condition and survival

Survival was 100 % under the control conditions. Under deoxygenation, survival decreased by 10 % (90 % survival), and under hypoxia, survival was significantly reduced by 31 % (69 % survival) compared to control ($p < 0.05$; Tables S2, S3, S5). EE displayed no mortality during the experiment; thus, the survival rate decreased only due to the mortality of LE (Fig. 2).

Development time (days post-laying; dpl) did not differ significantly across treatments. Moreover, the different experimental treatments did not affect the embryo wet mass, total length, or K (Fig. S1, Tables S3, S5).

3.2. Gene expression

In the head tissues of EE, hypoxia caused upregulation of *perf1* and *hif1a* compared to control ($p < 0.05$; Fig. 3; Tables S4, S5). The expression levels of *perf1* were also higher under hypoxia when compared to deoxygenation ($p < 0.05$; Fig. 3; Tables S4, S5). Additionally, the developmental stage played an important role in how hypoxia affected gene expression in the embryo's head tissue. Hypoxic LE exhibited significantly lower levels of *meltf, fer, perf1*, and *hif1a* compared to hypoxic EE ($0.01 < p < 0.05$; Fig. 3; Tables S4, S5).

In the trunk region, both immune and neuroendocrine responses were similar across treatments and developmental stages (see Supplementary Fig. S2; Tables S4, S5).

When analysing the overall response of the embryos (see Supplementary Fig. S3), we found that hypoxia caused the downregulation of *tnfr*, and deoxygenation caused the downregulation of *meltf* expression levels compared to the control ($p < 0.05$; Tables S3, S5).

Multivariate analysis (Fig. 4) showed that the first two dimensions of the principal component analysis (PCA) explained 74 % of the total variance, suggesting these two components explained the most significant proportion of variation and served as the primary axis for separating the treatment groups. PC1 and PC3 explained 62 % of the total variance, highlighting secondary patterns of variation in the selected neuroendocrine and immune-related genes. The individuals (replicates) were grouped by treatment: control, deoxygenation, and hypoxia, and the concentration ellipses represented the confidence intervals for each treatment group, indicating how distinct or overlapping these groups were in the PCA space. The iron metabolism genes (in blue) *fer*, *meltf*, and *fch*, focusing on how oxygen availability affects iron transport and storage, which are critical for cellular metabolism and immune function, the immune genes (in black), *lys*, *tnfr*, *perf1*, *nfkrf*, *irf2*, and *ifn,* reflecting immune responses under different oxygen levels, the neuroendocrine genes (in orange) *gh, ghr, mchr1, mchr2, tshr, thrb*, *tpo*, and *pomc,* representing hormonal regulation and stress-response changes, and the hypoxia-related gene *hif1a* (in grey) highlighting the impact of oxygen deprivation on cellular response, were differently loaded in each dimension. Fig. 4 showed that thyroid hormone signalling (*tshr, thrb*) and the growth hormone axis (*gh, ghr*) were tightly correlated. In contrast, *pomc* and *tpo* showed divergent behavior, likely reflecting neuroendocrine stress activation or hypoxia-modulated thyroid function. The PCA (Fig. 4) also suggested that the immune genes *perf1, irf2*, and *lys* were co-regulated with endocrine and iron metabolism genes, forming a homeostatic cluster, contrary to *ifn* that showed a negative correlation with *hif1a*, indicating it may decrease under hypoxia.

The first component (PC1; 53 % variance) primarily distinguished control samples, which clustered towards the negative axis, from deoxygenation samples, that were more centred on the PC, and hypoxia

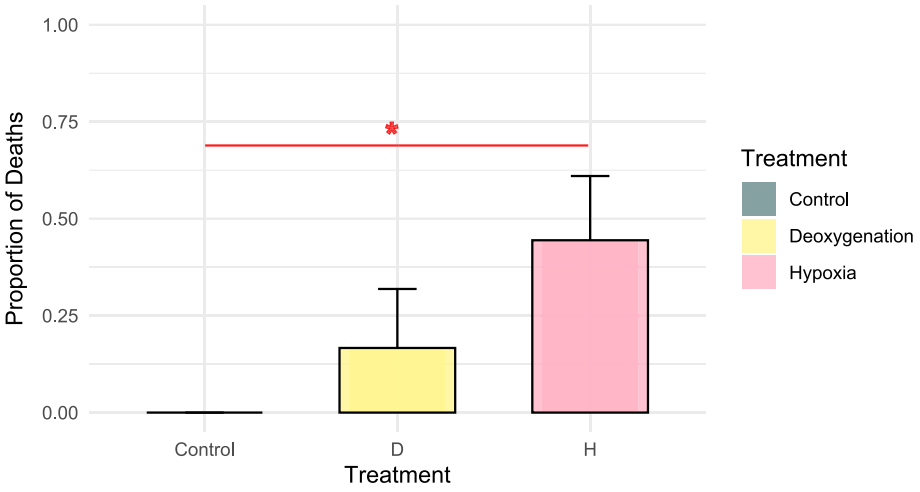

Fig. 2. The effect of treatment [control, deoxygenation (D), and hypoxia (H)] on the mortality proportion of small-spotted catshark late embryos (*Scyliorhinus canicula* LE; $n_{control} = 8$, $n_D = 6$, $n_H = 9$) after six days of exposure. No mortality occurred in the control treatment. Bars represent the mean proportion + standard error, calculated using binomial distribution. Significant differences between treatments are denoted by symbol superscripts ($p < 0.05$, Tables S3, S5).

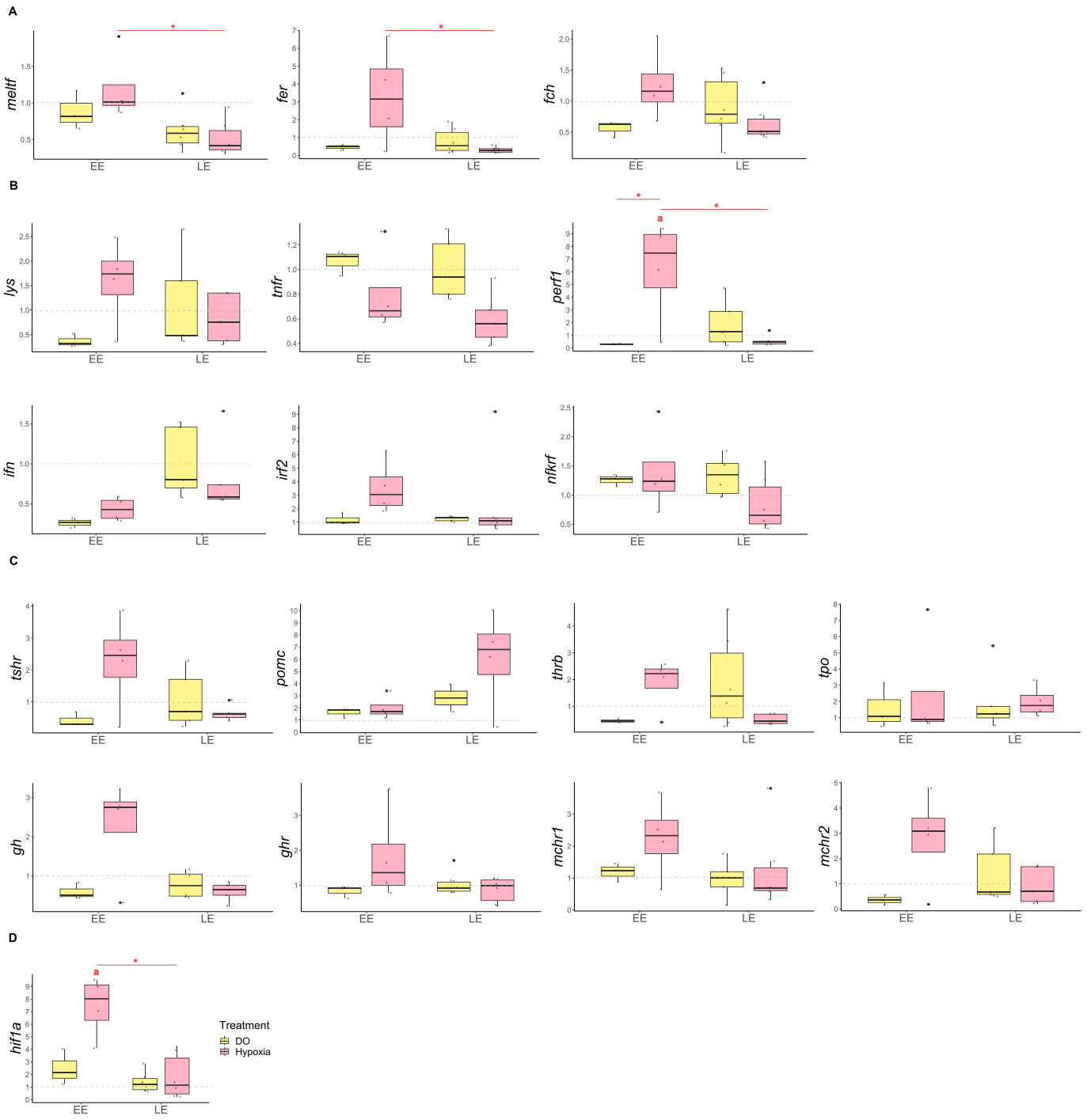

Fig. 3. Results of qPCR expression in head samples of early (EE) and late embryos (LE) of small-spotted catshark (*Scyliorhinus canicula*; $n_{control} = 11$, $n_D = 10$, $n_{Hypoxia} = 13$) after six days of exposure to deoxygenation (D; air saturation = 93 %) and hypoxia (H; air saturation = 26 %). A – iron metabolism (*meltf* – melanotransferrin, *fer* – ferritin heavy chain, *fch* – ferrochelatase); B – innate immune genes (*lys* – lysozyme G-like, *tnfr* – tumor necrosis factor receptor SF1A associated via death domain, *perf1* – perforin 1, *irf2* – interferon regulatory factor 2, *ifn* – interferon gamma-like, *nfkrf* – nuclear factor kappa B (NFKB) repressing factor); C – neuro-endocrine genes (*tshr* – TSH receptor, *thrb* – thyroid hormone receptor beta, *pomc* – proopiomelanocortin a, *tpo* – thyroid peroxidase, *gh* – growth hormone, *ghr* – growth hormone receptor, *mchr1,2* – melanin-concentrating hormone receptors 1 and 2), and D – hypoxia-related genes (*hif1a* – hypoxia-inducible factor 1 alpha). Expression levels were normalised using the geometric mean of ribosomal protein L13 (RPL13) and S29 (RPS29), and expressed as the fold change relative to the Control ($2^{-\Delta\Delta CT}$; 100 % of air saturation). Significant up or downregulation relative to the Control is denoted by letter superscripts ($p < 0.05$). Significant differences between D and hypoxia treatments are denoted by symbol superscripts ($p < 0.05$). Horizontal grey dashed lines represent the Control value (considered to be 1). Horizontal solid black lines represent the median, the whiskers represent the lowest and the highest values of the results, and the boundaries represent the 25th and 75th percentiles. Black dots represent outliers, and grey triangles represent individual data points. Additional statistical information is provided in Tables S4–5.

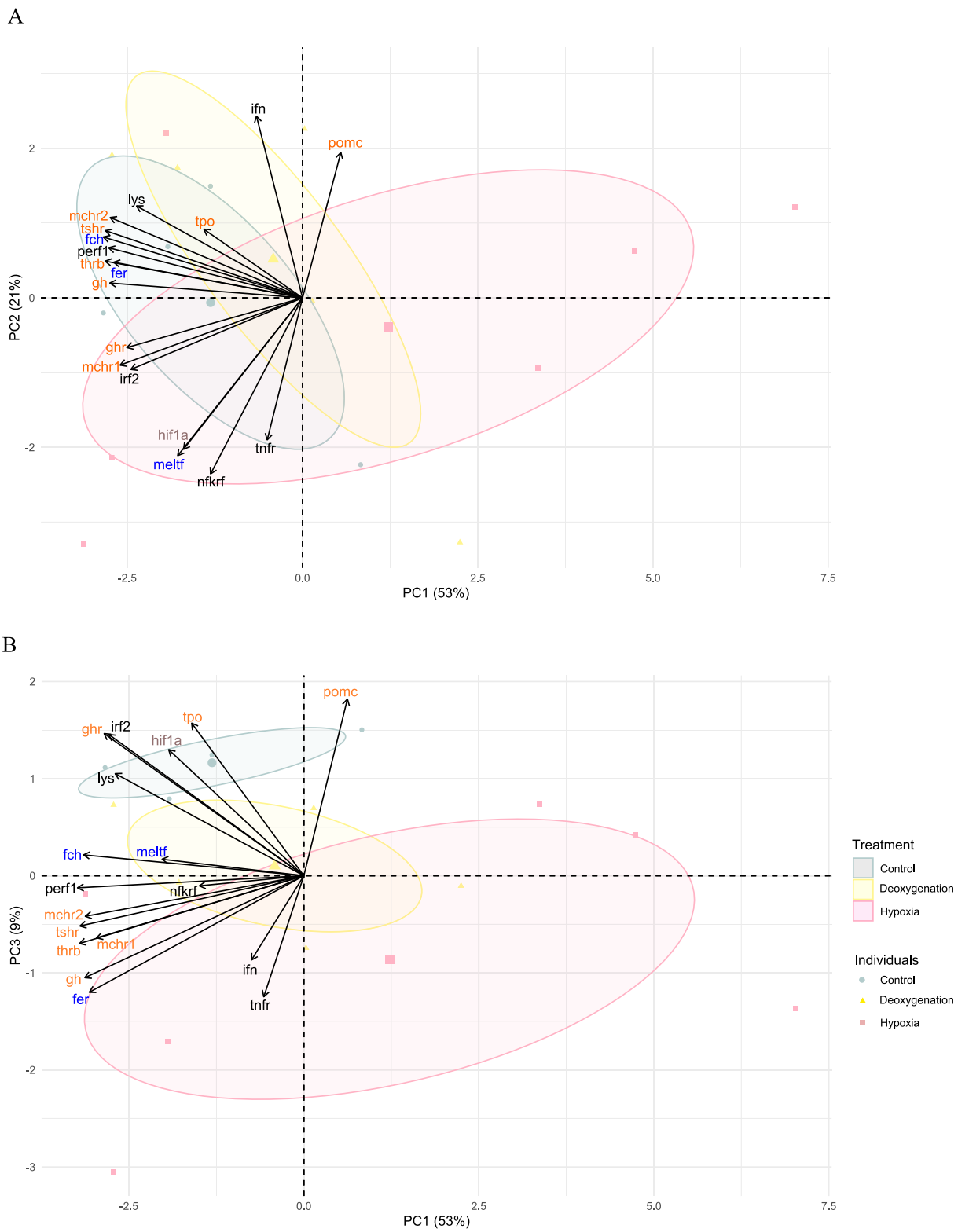

Fig. 4. Principal component analysis (PCA) biplot of individuals and variables. The individuals have been coloured according to the treatment [control, deoxygenation (D), and hypoxia (H)]. An individual refers to a replicate per treatment, variables are the gene expression of iron metabolism (blue: *fer*, *meltf*, *fch*), immune (black: *lys*, *tnfr*, *perf1*, *irf2*, *ifn*), neuroendocrine (orange: *gh*, *ghr*, *mchr1,2*, *tshr*, *thrb*, *pomc*), and hypoxia (grey: *hif1a*) related-genes, with concentration ellipses representing the confidence interval for each treatment. A – PC1 vs PC2 biplot; B – PC1 vs PC3 biplot. Despite PC3 explaining less overall variance than PC2, it effectively distinguished between the hypoxia and the control treatments, highlighting an expression pattern-specific treatment. (For interpretation of the references to colour in this figure legend, the reader is referred to the web version of this article.)

samples, positioned towards the positive axis. However, hypoxia was not strictly on the positive extreme, it overlapped with control and deoxygenation samples. This dimension suggested a suppression of biological responses in the control treatment, with strongly negatively loaded genes (between −0.92 and − 0.78) involved in iron metabolism (*fer* and *fch*), immune response (*perf1, irf2,* and *lys*), and neuroendocrine signalling (*gh, ghr, mchr1, mchr2, tshr,* and *thrb*). In contrast, DO treatment was associated with more neutral or mildly positive loadings, such as *pomc* (0.18), suggesting possible stress adaptation.

PC2 (21 % variance) mainly distinguished between the hypoxia treatment, located towards the negative axis, and the deoxygenation treatment, with samples loaded positively on PC2. Control samples were mostly intermediate between hypoxia and deoxygenation samples. The hypoxia treatment was characterised by high expression of iron transport, hypoxia-inducible, and inflammatory genes, such as *meltf, hif1a, nfkrf*, and *tnfr* (from − 0.77 to − 0.62), whereas the deoxygenation treatment was driven by immune genes, including *ifn* and *lys* (0.80 and 0.40, respectively).

PC3 (9 % variance) reflected divergent strategies, distinguishing the hypoxia treatment from the control. Although PC3 accounted for a smaller portion of total variance than PC2, it clearly separated samples from the hypoxia and control groups, highlighting a treatment-specific secondary expression pattern. Control treatment was characterised by the higher expression of genes associated with immune, endocrine and hypoxia inducible responses, such as *irf2, pomc, tpo, Sghr*, and *hif1a* (between 0.42 and 0.52), suggesting the activation of possible compensatory mechanisms that can support physiological stability and resilience when exposed to environmental variations. These responses may reflect anticipatory or adaptive adjustments that enable embryos to maintain growth, immune and endocrine function in dynamic coastal habitats where oxygen fluctuations may occur. In contrast, negatively loaded genes, associated with hypoxia, reflected reduced activity in growth and immune pathways, including *gh, fer*, and *tnfr* (around −0.35). The control group clustered with lower variability in gene expression, suggesting stable conditions, followed by deoxygenation and hypoxia groups, which showed more significant shifts along the principal components, reflecting changes in gene expression related to the stress response, iron metabolism, and immune regulation due to reduced oxygen availability.

4. Discussion

In the present study, mortality occurred only in late embryos (LE), both under deoxygenation (D) and hypoxic conditions (Figs. 2, 5). Although survival decreased by 10 %, shark embryos appeared to cope with the deoxygenation, as shown by the single alteration (decrease) in melanotransferrin (*meltf)* gene expression (Fig. 5, S3). Nevertheless, the decrease in *meltf* expression may pose developmental impairments to shark embryos under these conditions (further discussed). Under hypoxia, morphological/biometric data remained unaltered (Fig. S1), as previously reported by (Musa et al., 2020), and the expression levels of several genes were significantly changed (Fig. 5), suggesting some adaptive responses. Although the shark LE employed coping strategies, they were insufficient, resulting in a significant 31 % decrease in survival rate (Figs. 2, 5).

In stage four (EE), the inside of the shark's egg case may become

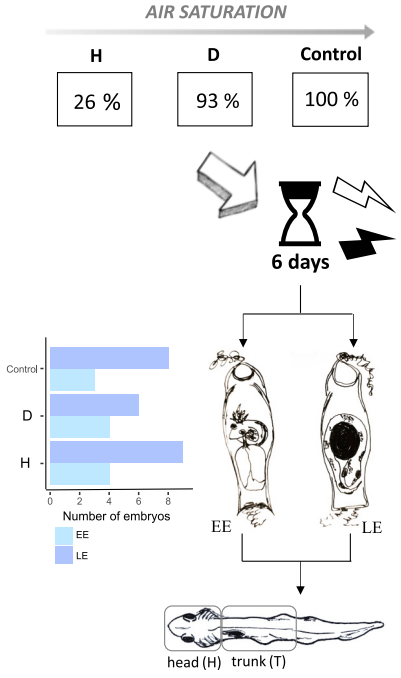

Compared to Control

	D	H	Model
SURVIVAL	=	↓ (LE)	***Treat*** + Dev. Stage
K	=	=	Treat + Dev. Stage
Weight	=	=	Treat + Dev. Stage
Length	=	=	Treat + Dev. Stage

GENE EXPRESSION compared to Control

Function	Gene	D	H	Hypoxia response LE compared to EE	Model
IM	*meltf*	↓	=	↓	***Treat * Dev. Stage***
	fer	=	=	↓	***Treat * Dev. Stage***
	fch	=	=	=	Treat * Dev. Stage
INN	*lys*	=	=	=	Treat * Dev. Stage
	tnfr	=	↓	=	Treat
	perf1	=	↑ (EE)	↓	***Treat * Dev. Stage***
	ifn	=	=	=	Treat + ***Dev. Stage***
	irf2	=	=	=	Treat * Dev. Stage
	nfkrf	=	=	=	Treat + Dev. Stage
END	*tshr*	=	=	=	Treat
	thrb	=	=	=	Treat * Dev. Stage
	pomc	=	=	=	Treat
	tpo	=	=	=	Treat
	gh	=	=	=	Treat * Dev. Stage
	ghr	=	=	=	Treat * Dev. Stage
	mchr1	=	=	=	Treat + Dev. Stage
	mchr2	=	=	=	Treat * Dev. Stage
HYP	*hif1a*	=	↑ (EE)	↓	***Treat * Dev. Stage***

Fig. 5. Immune and neuroendocrine response of small-spotted catshark were investigated after six days of exposure to deoxygenation (D) and hypoxic (H) conditions. Survival and Fulton condition factor (K) were calculated. Expression of genes related to iron metabolism (IM; *meltf*, *fer*, *fch*), the innate immune response (INN; *lys*, *tnfr*, *perf1*, *ifn*, *irf2*, *nfkrf*), neuroendocrine response (END; *tshr*, *thrb*, *pomc*, *tpo*, *gh*, *ghr*, *mchr1,2*), and hypoxia (HYP; *hif1a*) were quantified in the head (H) and trunk (T) of early (EE) and late (LE) embryos. Statistics are related to head samples, except for *tnfr* and *meltf*. Expression levels decreased ↓, increased ↑, or were maintained = compared to control. After determining whether the treatment, developmental stage, or tissue influenced each response variable, a model was fitted. The predictor variable that significantly affected the response variable is highlighted in italic bold ($p < 0.05$). The symbol * specifies interaction terms along with the main effects for those variables. Treat – treatment (control, D or hypoxia); Dev. Stage – developmental stage (EE or LE).

hypoxic (Rodda and Seymour, 2008) because the slits in the egg case are not completely opened and metabolic needs progressively increase (Musa et al., 2020; Rodda and Seymour, 2008). Some mechanisms, such as the external gills and the degradation of the jelly, provide improved access to oxygen (Musa et al., 2018), and the egg case porosity may facilitate respiratory exchanges (Goh et al., 2021). Together, these factors help early-stage embryos adapt to the low-oxygen microenvironment within the egg case. Once the egg case is opened (pre-hatching, LE), the egg case is inundated by the surrounding seawater and the inner microenvironment becomes normoxic, the gills are reabsorbed, and the metabolism is adjusted (Grunow et al., 2022; Musa et al., 2018).

When exposed to hypoxic environments, shark embryos may activate mechanisms to counteract hypoxia's potential stress and deleterious effects. One of the mechanisms is the adaptive response to hypoxia, which is mediated by an acute hypoxia-sensitive regulator, the transcription factor hypoxia-inducible factor 1 alpha (*hif1a*) (Lee and Tsai, 2017). This factor is a crucial regulator of cellular and systemic responses to low oxygen levels and a core protective response since it activates at least 1000 downstream target genes (Lee and Tsai, 2017; Tamamouna and Pitsouli, 2018). In many biological processes, including erythropoiesis, angiogenesis, metabolic reprogramming, cell-cycle regulation, and vascular remodelling *hif1a* has a key role (Gordan and Simon, 2007; Semenza, 2000). The positive correlation between *hif1a* and the control treatment observed in the PCA (Fig. 4) likely reflects a developmentally regulated role, as shown in early vascular and cardiac development (Semenza, 2000) in the context of the low oxygen environment inside the egg case (Rodda and Seymour, 2008). This interpretation is consistent with findings by Musa et al. (2018), who described progressive vascular growth during stages three and four of shark embryonic development. In contrast, the significant increase in *hif1a* gene expression in EE under hypoxic conditions compared to the control (Figs. 3, 5) confirms its role as a key mediator of the hypoxic response. This contrast underscores the dual role of *hif1a* during early embryogenesis (EE), which is to support normal development under baseline hypoxia, and facilitate physiological adjustments under environmental stress. Increased *hif1a* expression in hypoxia exposed EE suggests the embryos were well-adapted to low-oxygen environments. This aligns with the work of Rytkönen et al. (2012), who reported that in elasmobranchs, repeated or prolonged hypoxia increases *hif* mRNA levels, most likely to compensate for degradation of HIF proteins during extended periods of hypoxia. The variation in *hif1a* is related to the developmental phase of tissues or organs (Giaccia et al., 2004), suggesting it is influenced by the developmental stage of the organism. However, under hypoxic stress conditions, such as those experienced by LE in our study, the typical *hif1a* developmental pattern was disrupted (Figs. 3, 5). Specifically, LE exposed to hypoxia did not respond in the same way as EE and showed no significant differences in *hif1a* levels compared to the control group. This indicates that LE did not exhibit the expected protective response to the hypoxic conditions (Fig. 3). Furthermore, *hif1a* expression was lower in hypoxic LE compared to EE. The absence of this protective mechanism to hypoxia may explain the compromised LE survival under these conditions. Hypoxia-inducible factors are essential for fetal development and survival in mammals (Weidemann and Johnson, 2008), and the hypoxia signalling pathway is also established in early embryogenesis in zebrafish (Kajimura et al., 2006). *Hif1a* is suggested to regulate the activation of downstream genes (Lee and Tsai, 2017), and the PCA analysis (Fig. 4) revealed a positive correlation between *hif1a* and: *i)* some endocrine genes – *tpo, pomc*, and *ghr* – suggesting that hypoxia-related endocrine modulation may occur, possibly through thyroid and stress axis pathways; *ii)* all three iron metabolism genes, suggesting that hypoxia exposure is associated with altered iron metabolism, and may be essential to reallocate iron to essential pathways under limited oxygen; *iii)* most of the immune genes analysed – *perf1, irf2, lys, nfkrf*, and *tnfr* – which may support the notion of hypoxia-induced immune modulation. EE had increased expression levels of perforin 1 (*perf1*) in the head region, suggestive of enhanced innate immunity and improved efficiency of pathogen elimination (Tamura et al., 2008; Xu et al., 2021). In contrast, under hypoxia, LE decreased *perf1* gene expression compared to EE (Figs. 3, 5), suggesting reduced immune capacity, although LE may become more prone to infections due to increased exposure to seawater as the slits open. The expression level of the tumor necrosis factor receptor SF1A associated via death domain (*tnfr*) was downregulated and independent of the developmental stage (Fig. 5, S3). When inflammatory cytokines, such as tumor necrosis factor a (TNF-α), increase, the downstream effect is often an increase in the transcription of *hif1a* (Tamamouna and Pitsouli, 2018). Our results in developing sharks suggest the inverse process, as observed in LE exposed to hypoxia (Fig. 5). This may represent an immunological response to hypoxic stress (Yada and Tort, 2016) and may be a physiological trade-off (Sheldon and Verhulst, 1996).

Hypoxic LE had decreased expression levels of melanotransferrin (*meltf*) and ferritin heavy chain (*fer*) compared to hypoxic EE (Figs. 3, 5). The downregulation of *meltf* and *fer* – two of the three genes related to iron transport and storage – may suggest that these sharks' LE endured impairments in iron homeostasis. Ferritin has a major role in iron metabolism, and under conditions of iron deprivation (possibly caused by *meltf* decrease in hypoxic LE), its synthesis is repressed (Neves et al., 2009). In addition to the availability of oxygen, ferrous iron also regulates the HIF pathway (Giaccia et al., 2004). The modification in iron metabolism implied by the gene expression results in LE under hypoxia, may have compromised the activation of the HIF protective pathway. The results obtained for genes related to iron metabolism are coherent with other studies showing that hypoxia stress causes dysfunction in iron metabolism (Duarte et al., 2021). These two mechanisms highlight a biologically intricate feedback loop. Iron homeostasis is crucial for processes within the cell, including oxygen carrying, oxygen storage, energy production, or cellular metabolism, as well as for immune activation (Cronin et al., 2019). Furthermore, in hypoxic stress, iron homeostasis is fundamental to prevent cellular redox homeostasis impairment and for effective erythropoiesis during early vertebrate embryonic development (Hu et al., 2022; Zhang and Hamza, 2019). The possible compromised iron transport and storage may have exacerbated the effects of low oxygen and contributed to developmental impairments in LE. This is particularly important because iron metabolism plays a crucial role in DNA synthesis, cell division and growth, all of which are essential for normal embryonic development.

The downregulation of the innate elements *perf1* and *tnfr* and impairments in iron metabolism mechanisms (decreased *meltf* and *fer)* could have contributed to the mortality of LE under hypoxia. In fact, it is well described that low dissolved oxygen, or hypoxia, can negatively affect fish behavior, physiology, immunology, and growth (Abdel-Tawwab et al., 2019; Tamamouna and Pitsouli, 2018).

On the other hand, EE significantly increased the expression level of *hif1a*, which aligns with previous research that highlighted the critical role of *hif1a* in regulating hypoxia-induced genes responsible for innate immunity (Colgan et al., 2020; Lee and Tsai, 2017) and endocrine organ development (Wu et al., 2003), aiding in EE survival.

The significant differences observed in hypoxic head tissues (Fig. 3), contrary to hypoxic trunk tissues (Fig. S2), highlight the need to concentrate the analysis on specific tissues rather than on pooled tissues that may be a confounding factor and mark the organism's response to hypoxia. In the head, tissues such as the gills are in continuous direct contact with seawater and are the first tissue to experience hypoxia and may develop inflammation or systemic infections (Koppang et al., 2015; Li et al., 2022). Additionally, two primary lymphoid organs – the thymus and the Leydig organ – and the kidney are found in the anterior (head) region of *S. canicula* (Lloyd-Evans, 1993). This can support the increased expression level of *perf1* in the head samples. In contrast, the primary lymphoid organ – the epigonal organ – the spleen – a secondary lymphoid organ – and gut-associated lymphoid tissue (GALT) are located in the trunk (Lloyd-Evans, 1993; Rumfelt et al., 2002). However,

the epigonal organ and GALT do not appear until the pre-hatching stage (LE), and the spleen becomes organised into red and white pulp only in LE (Lloyd-Evans, 1993). This means that lymphoid tissues were negligible in trunk samples of EE, and therefore, the lack of responsive gene expression observed in the immune-related genes (Fig. S2).

These adaptive responses of shark embryos to hypoxic conditions may arise from either developmental plasticity or selection (Jonsson et al., 2022; Tobi et al., 2018). However, these responses are associated with long-term physiological changes in offspring. While plasticity may help offspring to better cope with extreme environmental events in later stages, selection may lead to diminished health in adults (Jonsson et al., 2022; Tobi et al., 2018). Thus, distinguishing between genetic adaptations and phenotypic plasticity under environmental influences warrants further investigation.

5. Conclusion

The activation of the HIF pathway in EE, which did not suffer any mortality under hypoxia, suggests that this pathway was essential in their survival. In contrast, some LE of *S. canicula* were resilient and modified pathways to cope with the loss of oxygen. However, a survival rate of 69 % may indicate there is a threshold beyond which the animals cannot cope with hypoxia stress. The energetic trade-offs faced by shark LE in response to hypoxia suggests they must allocate energy towards essential physiological processes while managing the constraints imposed by reduced oxygen availability, while these older embryos face an increase in oxygen demand due to their increase in tissue mass (Musa et al., 2020; Rodda and Seymour, 2008). The apparent lack of an effective protective response to hypoxia in LE – decreased *hif1a* expression – may centre on these energetic trade-offs and may have resulted in the reduced survival of these embryos. This may have been compounded by impaired iron homeostasis (implied by decreased *meltf* and *fer* gene expression) and the effort to maintain growth similar to that of control LE, resulting in higher mortality under hypoxia. Our study underscored the balance that shark LE must strike between immediate survival and long-term developmental success in low-oxygen environments. In further studies, an increased number of animals might lead to a more homogenous response, reducing individual variability present in the recorded physiological responses. This would improve study power and practical significance, while minimising type II errors, potentially revealing additional response mechanisms. The identification of biological patterns and underlying pathways is essential for understanding and predicting ecological processes, including climate change effects (Clarke, 2017; Dahlke et al., 2020). Because hypoxia limits energy acquisition, exposure to additional stressors may push small-spotted catsharks beyond the “tipping point” of the adaptive responses, exacerbating the effects of co-occurring stressors that increase energy demands (Diaz et al., 2019), and enhancing the negative impact on survival. Thus, the selective responses and decreased survival of small-spotted catshark embryos can potentially lead to population decline, threaten this species’ population dynamics, impair its ecological role as a mesopredator, and disrupt ecosystem balance in temperate regions. Future studies should evaluate other signalling pathways, such as AMPK, MAPK, and IGF/PI3K/Akt, that regulate oxygen-sensitive transcription (Zhu et al., 2013). Analysing enzymes involved in glycolysis would also be essential due to their role in hypoxia adaptation. Lastly, further studies using transcriptomic or proteomic sequencing may reveal additional mechanisms involved in the response of developing sharks to hypoxia.

Supplementary data to this article can be found online at https://doi.org/10.1016/j.cbpa.2025.111904.

CRediT authorship contribution statement

Sandra Martins: Writing – review & editing, Writing – original draft, Visualization, Validation, Methodology, Investigation, Formal analysis, Data curation, Conceptualization. **Jaquelino Varela:** Methodology. **Rute Felix:** Writing – review & editing, Validation, Supervision, Resources, Methodology. **Catarina Pereira Santos:** Methodology, Investigation. **José Ricardo Paula:** Writing – review & editing, Methodology, Funding acquisition. **Deborah M. Power:** Writing – review & editing, Writing – original draft, Validation, Supervision, Resources, Project administration, Methodology, Funding acquisition, Conceptualization. **Rui Rosa:** Writing – review & editing, Writing – original draft, Validation, Supervision, Resources, Project administration, Methodology, Funding acquisition, Conceptualization.

Declaration of competing interest

None.

Data availability

Research data can be consulted in the link https://data.mendeley.com/datasets/sksz3648np/2

Acknowledgements

The authors are very grateful to Aquário Vasco da Gama (AVG, Portugal) for providing small-spotted catshark embryos, to Melanie Marques from Laboratório Marítimo da Guia (MARE/FCUL, Portugal) for providing the basis for the R script for the statistical analysis, and to the bachelor student (FCUL, Portugal) Ana Carolina Silva for her willingness to help in the final sampling.

This study was supported by Fundação para a Ciência e Tecnologia (FCT), through the strategic project UID/MAR/04292/2020 granted to MARE, the project LA/P/0069/2020 granted to the Associate Laboratory ARNET, the project Ascend (PTDC/BIA-BMA/28609/2017), Ph.D grants to SM (SFRH/BD/145276/2019; COVID/BD/153548/2024) and CS (SFRH/BD/117890/ 2016). JRP was supported by the fellowship”la Caixa” Foundation (ID 100010434) code 142382. CCMAR was supported by FCT strategic projects UIDB/04326/ 2020 (DOI:10.54499/UIDB/04326/2020), UIDP/04326/2020 (DOI:10 0.54499/UIDP/04326/ 2020), and LA/P/0101/2020 (DOI:10.54499/ LA/P/0101/2020), and the operational programs CRESC Algarve 2020 and COMPETE 2020 through projects EMBRC.PT ALG-01- 0145-FEDER-022121. Program MAR2020 also supported this study through the project TUBAREPEL (MAR-01.04.02-FEAMP-0006). Prince Albert II of Monaco Foundation, Intergovernmental Panel on Climate Change (IPCC), and O Camões – Instituto da Cooperação e da Língua, I.P. supported JV Ph.D. grant.

References

Abdel-Tawwab, M., Monier, M.N., Hoseinifar, S.H., Faggio, C., 2019. Fish response to hypoxia stress: growth, physiological, and immunological biomarkers. Fish Physiol. Biochem. 45, 997–1013. https://doi.org/10.1007/s10695-019-00614-9.

Aku, P., Tonn, W.M., 1997. Changes in population structure, growth, and biomass of cisco (Coregonus artedi) during hypolimnetic oxygenation of a deep, eutrophic Lake, Amisk Lake Alberta. Can. J. Fish. Aquat. Sci. 54, 2196–2206. https://doi.org/10.1139/f97-118.

Balasch, J.C., Tort, L., 2019. Netting the stress responses in fish. Front. Endocrinol. 10.

Barton, B.A., 2002. Stress in fishes: a diversity of responses with particular reference to changes in circulating corticosteroids. Integr. Comp. Biol. 42, 517–525. https://doi.org/10.1093/icb/42.3.517.

Brandt, S.B., Costantini, M., Kolesar, S., Ludsin, S.A., Mason, D.M., Rae, C.M., Zhang, H., 2011. Does hypoxia reduce habitat quality for Lake Erie walleye (Sander vitreus)? A bioenergetics perspective. Can. J. Fish. Aquat. Sci. 68, 857–879. https://doi.org/10.1139/f2011-018.

Breitburg, D., Levin, L.A., Oschlies, A., Grégoire, M., Chavez, F.P., Conley, D.J., Garçon, V., Gilbert, D., Gutiérrez, D., Isensee, K., Jacinto, G.S., Limburg, K.E., Montes, I., Naqvi, S.W.A., Pitcher, G.C., Rabalais, N.N., Roman, M.R., Rose, K.A., Seibel, B.A., Telszewski, M., Yasuhara, M., Zhang, J., 2018. Declining oxygen in the global ocean and coastal waters. Science 359, eaam7240. https://doi.org/10.1126/science.aam7240.

Childress, J.J., Seibel, B.A., 1998. Life at stable low oxygen levels: adaptations of animals to oceanic oxygen minimum layers. J. Exp. Biol. 201, 1223–1232. https://doi.org/10.1242/jeb.201.8.1223.

Clarke, A., 2017. Energy and heat. In: Clarke, A. (Ed.), Principles of Thermal Ecology: Temperature, Energy, and Life. Oxford University Press, p. 0. https://doi.org/10.1093/oso/9780199551668.003.0002.

Colgan, S.P., Furuta, G.T., Taylor, C.T., 2020. Hypoxia and innate immunity: keeping up with the HIFsters. Annu. Rev. Immunol. 38, 341–363. https://doi.org/10.1146/annurev-immunol-100819-121537.

Compagno, L.V.J., 1984. Part 2. Carcharhiniformes. In: An Annotated and Illustrated Catalogue of Shark Species Known to Date, FAO SPECIES CATALOGUE. Rome.

Craig, J., Crowder, L., 2005. Hypoxia-induced habitat shifts and energetic consequences in Atlantic croaker and brown shrimp on the Gulf of Mexico shelf. Mar. Ecol. Prog. Ser. 294, 79–94. https://doi.org/10.3354/meps294079.

Cronin, S.J.F., Woolf, C.J., Weiss, G., Penninger, J.M., 2019. The role of Iron regulation in Immunometabolism and immune-related disease. Front. Mol. Biosci. 6, 116. https://doi.org/10.3389/fmolb.2019.00116.

Dahlke, F.T., Wohlrab, S., Butzin, M., Pörtner, H.-O., 2020. Thermal bottlenecks in the life cycle define climate vulnerability of fish. Science 369, 65–70. https://doi.org/10.1126/science.aaz3658.

Dam, H.G., 2013. Evolutionary adaptation of marine zooplankton to global change. Annu. Rev. Mar. Sci. 5, 349–370. https://doi.org/10.1146/annurev-marine-121211-172229.

Diaz, R.J., Rosenberg, R., Sturdivant, K., 2019. Hypoxia in estuaries and semi- enclosed seas. In: Ocean Deoxygenation: Everyone's Problem. IUCN, Gland, Switzerland.

Diez, J.M., Davenport, J., 1990. Energy exchange between the yolk and embryo of dogfish (scyliorhinus canicula L.) eggs held under normoxic, hypoxic and transient anoxic conditions. Comparat. Biochem. Physiol. Part B: Compar. Biochem. 96, 825–830. https://doi.org/10.1016/0305-0491(90)90239-P.

Duarte, T.L., Talbot, N.P., Drakesmith, H., 2021. NRF2 and hypoxia-inducible factors: key players in the redox control of systemic Iron homeostasis. Antioxid. Redox Signal. 35, 433–452. https://doi.org/10.1089/ars.2020.8148.

Eby, L., Crowder, L., McClellan, C., Peterson, C., Powers, M., 2005. Habitat degradation from intermittent hypoxia: impacts on demersal fishes. Mar. Ecol. Prog. Ser. 291, 249–262. https://doi.org/10.3354/meps291249.

Ellis, J.R., Shackley, S.E., 1997. The reproductive biology of Scyliorhinus canicula in the Bristol Channel, U.K. J. Fish Biol. 51, 361–372. https://doi.org/10.1111/j.1095-8649.1997.tb01672.x.

Giaccia, A.J., Simon, M.C., Johnson, R., 2004. The biology of hypoxia: the role of oxygen sensing in development, normal function, and disease. Genes Dev. 18, 2183–2194. https://doi.org/10.1101/gad.1243304.

Goh, R., Danielsen, S.P.O., Schaible, E., McMeeking, R.M., Waite, J.H., 2021. Nanolatticed architecture mitigates damage in shark egg cases. Nano Lett. 21, 8080–8085. https://doi.org/10.1021/acs.nanolett.1c02439.

Gordan, J.D., Simon, M.C., 2007. Hypoxia-inducible factors: central regulators of the tumor phenotype. Curr. Opin. Genet. Dev. 17, 71–77. https://doi.org/10.1016/j.gde.2006.12.006.

Gorissen, M., Flik, G., 2016. 3 The endocrinology of the stress response in fish: An adaptation-physiological view. In: Schreck, C.B., Tort, L., Farrell, A.P., Brauner, C.J. (Eds.), Fish Physiology, Biology of Stress in Fish. Academic Press, pp. 75–111. https://doi.org/10.1016/B978-0-12-802728-8.00003-5.

Greijer, A., van der Groep, P., Kemming, D., Shvarts, A., Semenza, G., Meijer, G., van de Wiel, M., Belien, J., van Diest, P., van der Wall, E., 2005. Up-regulation of gene expression by hypoxia is mediated predominantly by hypoxia-inducible factor 1 (HIF-1). J. Pathol. 206, 291–304. https://doi.org/10.1002/path.1778.

Grunow, B., Reismann, T., Moritz, T., 2022. Pre-hatching ontogenetic changes of morphological characters of small-spotted catshark (Scyliorhinus canicula). Fishes 7, 100. https://doi.org/10.3390/fishes7030100.

Hazon, N., Wells, A., Pillans, R.D., Good, J.P., Gary Anderson, W., Franklin, C.E., 2003. Urea based osmoregulation and endocrine control in elasmobranch fish with special reference to euryhalinity. Comp. Biochem. Physiol. B: Biochem. Mol. Biol. 136, 685–700. https://doi.org/10.1016/S1096-4959(03)00280-X.

Hu, R., Li, G., Xu, Q., Chen, L., 2022. Iron supplementation inhibits hypoxia-induced mitochondrial damage and protects zebrafish liver cells from death. Front. Physiol. 13. https://doi.org/10.3389/fphys.2022.925752.

IPCC, 2019. Climate Change and Land: an IPCC special report on climate change, desertification, land degradation, sustainable land management, food security, and greenhouse gas fluxes in terrestrial ecosystems. In: Shukla, P.R., Skea, J., Buendia, E. Calvo, Masson-Delmotte, V., Pörtner, H.-O., Roberts, D.C., Zhai, P., Slade, R., Connors, S., van Diemen, R., Ferrat, M., Haughey, E., Luz, S., Neogi, S., Pathak, M., Petzold, J., Pereira, J. Portugal, Vyas, P., Huntley, E., Kissick, K., Belkacemi, M., Malley, J. (Eds.), Intergovernmental Panel on Climate Change (IPCC).

IPCC, 2023. Climate change 2023: synthesis report. Contribution of working groups I, II and III to the sixth assessment report of the intergovernmental panel on climate change, Core writing team. In: Lee, H., Romero, J. (Eds.), Intergovernmental panel on climate change (IPCC), Geneva, Switzerland. https://doi.org/10.59327/IPCC/AR6-9789291691647.

Jonsson, B., Jonsson, N., Hansen, M.M., 2022. Knock-on effects of environmental influences during embryonic development of ectothermic vertebrates. Q. Rev. Biol. 97, 95–139. https://doi.org/10.1086/720081.

Kajimura, S., Aida, K., Duan, C., 2006. Understanding hypoxia-induced gene expression in early development: in vitro and in vivo analysis of hypoxia-inducible factor 1-regulated zebra fish insulin-like growth factor binding protein 1 gene expression. Mol. Cell. Biol. 26, 1142–1155. https://doi.org/10.1128/MCB.26.3.1142-1155.2006.

Khansari, A.R., Balasch, J., Reyes-López, F., Tort, L., 2017. Stressing the inflammatory network: Immuno-endocrine responses to allostatic load in fish. J. Mar. Sci. Technol. 1, 1–14.

Koppang, E.O., Kvellestad, A., Fischer, U., 2015. 5 Fish mucosal immunity: Gill. In: Beck, B.H., Peatman, E. (Eds.), Mucosal Health in Aquaculture. Academic Press, San Diego, pp. 93–133. https://doi.org/10.1016/B978-0-12-417186-2.00005-4.

Kvamme, B.O., Gadan, K., Finne-Fridell, F., Niklasson, L., Sundh, H., Sundell, K., Taranger, G.L., Evensen, Ø., 2013. Modulation of innate immune responses in Atlantic salmon by chronic hypoxia-induced stress. Fish Shellfish Immunol. 34, 55–65. https://doi.org/10.1016/j.fsi.2012.10.006.

Laffoley, D., Baxter, J.M., 2019. Ocean Deoxygenation: Everyone's Problem Causes, Impacts, Consequences and Solutions., Full Report. IUCN, Gland, Switzerland.

Lee, H.-C., Tsai, S.-J., 2017. Endocrine targets of hypoxia-inducible factors. J. Endocrinol. 234, R53–R65. https://doi.org/10.1530/JOE-16-0653.

Li, X., Ling, C., Wang, Q., Feng, C., Luo, X., Sha, H., He, G., Zou, G., Liang, H., 2022. Hypoxia stress induces tissue damage, immune defense, and oxygen transport change in gill of silver carp (Hypophthalmichthys molitrix): evaluation on hypoxia by using transcriptomics. Front. Mar. Sci. 9. https://doi.org/10.3389/fmars.2022.900200.

Limburg, K.E., Breitburg, D., Swaney, D.P., Jacinto, G., 2020. Ocean deoxygenation: a primer. One Earth 2, 24–29. https://doi.org/10.1016/j.oneear.2020.01.001.

Livak, K.J., Schmittgen, T.D., 2001. Analysis of relative gene expression data using real-time quantitative PCR and the 2−ΔΔCT method. Methods 25, 402–408. https://doi.org/10.1006/meth.2001.1262.

Lloyd-Evans, P., 1993. Development of the lymphomyeloid system in the dogfish, Scyliorhinus canicula. Dev. Comp. Immunol. 17, 501–514. https://doi.org/10.1016/S0145-305X(05)80006-0.

Machado, M., Malheiro, D., Couto, A., Wilson, J.M., Guerreiro, M., Azeredo, R., Svendsen, J.C., Afonso, A., Serradeiro, R., Costas, B., 2018. Acute hyperoxia induces systemic responses with no major changes in peripheral tissues in the Senegalese sole (Solea senegalensis Kaup, 1858). Fish Shellfish Immunol. 74, 260–267. https://doi.org/10.1016/j.fsi.2018.01.008.

Makrinos, D.L., Bowden, T.J., 2016. Natural environmental impacts on teleost immune function. Fish Shellfish Immunol. 53, 50–57. https://doi.org/10.1016/j.fsi.2016.03.008.

Martins, S., Ferreira, C., Mateus, A.P., Santos, C.P., Fonseca, J., Rosa, R., Power, D.M., 2024. Immunological resilience of a temperate catshark to a simulated marine heat wave. J. Exp. Biol. https://doi.org/10.1242/jeb.247684.

McBryan, T.L., Anttila, K., Healy, T.M., Schulte, P.M., 2013. Responses to temperature and hypoxia as interacting stressors in fish: implications for adaptation to environmental change. Integr. Comp. Biol. 53, 648–659. https://doi.org/10.1093/icb/ict066.

Methling, C., Aluru, N., Vijayan, M.M., Steffensen, J.F., 2010. Effect of moderate hypoxia at three acclimation temperatures on stress responses in Atlantic cod with different haemoglobin types. Comp. Biochem. Physiol. A Mol. Integr. Physiol. 156, 485–490. https://doi.org/10.1016/j.cbpa.2010.04.006.

Mucha, S., 2023. Behavioral activity and hypoxia tolerance of African weakly electric fish (doctoralThesis). Humboldt-Universität zu Berlin. https://doi.org/10.18452/25649.

Musa, S.M., Czachur, M.V., Shiels, H.A., 2018. Oviparous elasmobranch development inside the egg case in 7 key stages. PLoS One 13, e0206984. https://doi.org/10.1371/journal.pone.0206984.

Musa, S.M., Ripley, D.M., Moritz, T., Shiels, H.A., 2020. Ocean warming and hypoxia affect embryonic growth, fitness and survival of small-spotted catsharks, Scyliorhinus canicula. J. Fish Biol. 97, 257–264. https://doi.org/10.1111/jfb.14370.

Neves, J.V., Wilson, J.M., Rodrigues, P.N.S., 2009. Transferrin and ferritin response to bacterial infection: the role of the liver and brain in fish. Dev. Comp. Immunol. 33, 848–857. https://doi.org/10.1016/j.dci.2009.02.001.

Niklasson, L., Sundh, H., Fridell, F., Taranger, G.L., Sundell, K., 2011. Disturbance of the intestinal mucosal immune system of farmed Atlantic salmon (Salmo salar), in response to long-term hypoxic conditions. Fish Shellfish Immunol. 31, 1072–1080. https://doi.org/10.1016/j.fsi.2011.09.011.

Pegado, M.R., Santos, C.P., Pimentel, M., Cyrne, R., Paulo, M., Maulvaut, A.L., Raffoul, D., Diniz, M., Bispo, R., Rosa, R., 2020a. Effects of elevated carbon dioxide on the hematological parameters of a temperate catshark. J. Exp. Zool. Part A: Ecolog. Integrat. Physiol. 333, 126–132. https://doi.org/10.1002/jez.2333.

Pegado, M.R., Santos, C.P., Raffoul, D., Konieczna, M., Sampaio, E., Luísa Maulvault, A., Diniz, M., Rosa, R., 2020b. Impact of a simulated marine heatwave in the hematological profile of a temperate shark (Scyliorhinus canicula). Ecol. Indic. 114, 106327. https://doi.org/10.1016/j.ecolind.2020.106327.

Power, D.M., Llewellyn, L., Faustino, M., Nowell, M.A., Björnsson, B.T., Einarsdottir, I.E., Canario, A.V., Sweeney, G.E., 2001. Thyroid hormones in growth and development of fish. Comp Biochem Physiol C Toxicol Pharmacol 130, 447–459. https://doi.org/10.1016/s1532-0456(01)00271-x.

Ricker, W.E., 1975. Computation and Interpretation of Biological Statistics of Fish Populations, vol. No. 191. Bulletin of the Fisheries Research Board of Canada.

Rodda, K.R., Seymour, R.S., 2008. Functional morphology of embryonic development in the port Jackson shark Heterodontus portusjacksoni (Meyer). J. Fish Biol. 72, 961–984. https://doi.org/10.1111/j.1095-8649.2007.01777.x.

Roman, M.R., Brandt, S.B., Houde, E.D., Pierson, J.J., 2019. Interactive effects of hypoxia and temperature on coastal pelagic zooplankton and fish. Frontiers in marine. Science 6.

Rosa, R., Baptista, M., Lopes, V.M., Pegado, M.R., Ricardo Paula, J., Trübenbach, K., Leal, M.C., Calado, R., Repolho, T., 2014. Early-life exposure to climate change impairs tropical shark survival. Proc. R. Soc. B Biol. Sci. 281, 20141738. https://doi.org/10.1098/rspb.2014.1738.

Rosa, R., Ricardo Paula, J., Sampaio, E., Pimentel, M., Lopes, A.R., Baptista, M., Guerreiro, M., Santos, C., Campos, D., Almeida-Val, V.M.F., Calado, R., Diniz, M., Repolho, T., 2016. Neuro-oxidative damage and aerobic potential loss of sharks under elevated CO2 and warming. Mar. Biol. 163, 119. https://doi.org/10.1007/s00227-016-2898-7.

Rumfelt, L.L., McKINNEY, E.C., Taylor, E., Flajnik, M.F., 2002. The development of primary and secondary lymphoid tissues in the nurse shark Ginglymostoma cirratum: B-cell zones precede dendritic cell immigration and T-cell zone formation during ontogeny of the spleen. Scand. J. Immunol. 56, 130–148. https://doi.org/10.1046/j.1365-3083.2002.01116.x.

Rytkönen, K.T., Renshaw, G.M.C., Vainio, P.P., Ashton, K.J., Williams-Pritchard, G., Leder, E.H., Nikinmaa, M., 2012. Transcriptional responses to hypoxia are enhanced by recurrent hypoxia (hypoxic preconditioning) in the epaulette shark. Physiol. Genomics 44, 1090–1097. https://doi.org/10.1152/physiolgenomics.00081.2012.

Sampaio, E., Santos, C., Rosa, I.C., Ferreira, V., Pörtner, H.-O., Duarte, C.M., Levin, L.A., Rosa, R., 2021. Impacts of hypoxic events surpass those of future ocean warming and acidification. Nat Ecol Evol 5, 311–321. https://doi.org/10.1038/s41559-020-01370-3.

Santos, C.P., Sampaio, E., Pereira, B.P., Pegado, M.R., Borges, F.O., Wheeler, C.R., Bouyoucos, I.A., Rummer, J.L., Frazão Santos, C., Rosa, R., 2021. Elasmobranch responses to experimental warming, acidification, and oxygen loss—a Meta-analysis. Front. Mar. Sci. 8, 735377.

Sapolsky, R.M., Romero, L.M., Munck, A.U., 2000. How do glucocorticoids influence stress responses? Integrating permissive, suppressive, stimulatory, and preparative actions. Endocr. Rev. 21, 55–89. https://doi.org/10.1210/edrv.21.1.0389.

Semenza, G.L., 2000. HIF-1: mediator of physiological and pathophysiological responses to hypoxia. J. Appl. Physiol. 1985 (88), 1474–1480. https://doi.org/10.1152/jappl.2000.88.4.1474.

Shang, E.H.H., Wu, R.S.S., 2004. Aquatic hypoxia is a teratogen and affects fish embryonic development. Environ. Sci. Technol. 38, 4763–4767. https://doi.org/10.1021/es0496423.

Sheldon, B.C., Verhulst, S., 1996. Ecological immunology: costly parasite defences and trade-offs in evolutionary ecology. Trends Ecol. Evol. 11, 317–321. https://doi.org/10.1016/0169-5347(96)10039-2.

Tamamouna, V., Pitsouli, C., 2018. The hypoxia-inducible factor-1α in angiogenesis and Cancer: insights from the Drosophila model, in: gene expression and regulation in mammalian cells transcription toward the establishment of novel therapeutics. IntechOpen. https://doi.org/10.5772/intechopen.72318.

Tamura, T., Yanai, H., Savitsky, D., Taniguchi, T., 2008. The IRF family transcription factors in immunity and oncogenesis. Annu. Rev. Immunol. 26, 535–584. https://doi.org/10.1146/annurev.immunol.26.021607.090400.

Tavares, L., Alves, P.M., Ferreira, R.B., Santos, C.N., 2011. Comparison of different methods for DNA-free RNA isolation from SK-N-MC neuroblastoma. BMC. Res. Notes 4, 3. https://doi.org/10.1186/1756-0500-4-3.

Taylor, J.C., Miller, J.M., 2001. Physiological performance of juvenile southern flounder, Paralichthys lethostigma (Jordan and Gilbert, 1884), in chronic and episodic hypoxia. J. Exp. Mar. Biol. Ecol. 258, 195–214. https://doi.org/10.1016/s0022-0981(01)00215-5.

Thomas, P., Rahman, M.S., 2012. Extensive reproductive disruption, ovarian masculinization and aromatase suppression in Atlantic croaker in the northern Gulf of Mexico hypoxic zone. Proc. Biol. Sci. 279, 28–38. https://doi.org/10.1098/rspb.2011.0529.

Thomas, P., Rahman, Md.S., Khan, I.A., Kummer, J.A., 2007. Widespread endocrine disruption and reproductive impairment in an estuarine fish population exposed to seasonal hypoxia. Proc. Biol. Sci. 274, 2693–2702. https://doi.org/10.1098/rspb.2007.0921.

Tobi, E.W., van den Heuvel, J., Zwaan, B.J., Lumey, L.H., Heijmans, B.T., Uller, T., 2018. Selective survival of embryos can explain DNA methylation signatures of adverse prenatal environments. Cell Rep. 25, 2660–2667.e4. https://doi.org/10.1016/j.celrep.2018.11.023.

Vaquer-Sunyer, R., Duarte, C.M., 2008. Thresholds of hypoxia for marine biodiversity. Proc. Natl. Acad. Sci. 105, 15452–15457. https://doi.org/10.1073/pnas.0803833105.

Varela, J., Martins, S., Court, M., Santos, C.P., Paula, J.R., Ferreira, I.J., Diniz, M., Repolho, T., Rosa, R., 2023. Impacts of deoxygenation and hypoxia on shark embryos anti-predator behavior and oxidative stress. Biology 12, 577. https://doi.org/10.3390/biology12040577.

Virtanen, M.I., Brinchmann, M.F., Patel, D.M., Iversen, M.H., 2023. Chronic stress negatively impacts wound healing, welfare, and stress regulation in internally tagged Atlantic salmon (Salmo salar). Front. Physiol. 14.

Weidemann, A., Johnson, R.S., 2008. Biology of HIF-1alpha. Cell Death Differ. 15, 621–627. https://doi.org/10.1038/cdd.2008.12.

Wendelaar Bonga, S.E., 1997. The stress response in fish. Physiol. Rev. 77, 591–625. https://doi.org/10.1152/physrev.1997.77.3.591.

Wheeler, C.R., Gervais, C.R., Johnson, M.S., Vance, S., Rosa, R., Mandelman, J.W., Rummer, J.L., 2020. Anthropogenic stressors influence reproduction and development in elasmobranch fishes. Rev. Fish Biol. Fish. 30, 373–386. https://doi.org/10.1007/s11160-020-09604-0.

Wood, C.M., Giacomin, M., 2016. Feeding through your gills and turning a toxicant into a resource: how the dogfish shark scavenges ammonia from its environment. J. Exp. Biol. 219, 3218–3226. https://doi.org/10.1242/jeb.145268.

Wu, R.S.S., Zhou, B.S., Randall, D.J., Woo, N.Y.S., Lam, P.K.S., 2003. Aquatic hypoxia is an endocrine disruptor and impairs fish reproduction. Environ. Sci. Technol. 37, 1137–1141. https://doi.org/10.1021/es0258327.

Xu, J., Yang, N., Xie, T., Yang, G., Chang, L., Yan, D., Li, T., 2021. Summary and comparison of the perforin in teleosts and mammals: a review. Scand. J. Immunol. 94, e13047. https://doi.org/10.1111/sji.13047.

Yada, T., Tort, L., 2016. Stress and disease resistance: immune system and Immunoendocrine. Interactions 35, 365–403. https://doi.org/10.1016/B978-0-12-802728-8.00010-2.

Zhang, J., Hamza, I., 2019. Ze brafish as a model system to delineate the role of heme and iron metabolism during erythropoiesis. Mol. Genet. Metab. 128, 204–212. https://doi.org/10.1016/j.ymgme.2018.12.007.

Zhang, H., Mason, D., Stow, C., Adamack, A., Brandt, S., Zhang, X., Kimmel, D., Roman, M., Boicourt, W., Ludsin, S., 2014. Effects of hypoxia on habitat quality of pelagic planktivorous fishes in the northern Gulf of Mexico. Mar. Ecol. Prog. Ser. 505, 209–226. https://doi.org/10.3354/meps10768.

Zhu, C.-D., Wang, Z.-H., Yan, B., 2013. Strategies for hypoxia adaptation in fish species: a review. J. Comp. Physiol. B. 183, 1005–1013. https://doi.org/10.1007/s00360-013-0762-3.